文章编号：1001-9014(2024)05-0628-06

DOI:10.11972/j.issn.1001-9014.2024.05.007

Dual-band multi-beam reconfigurable terahertz antenna based on graphene frequency selective surface

JIN Zhao[1], RONG Yu[1*], QIAO Li-Ping[2*], YU Jing-Dong[1], WU Fei[1], GUO Chen[1], TIAN Dou[1]

(1. School of Information Engineering, Chang'an University, Xi'an 710064, China;
2. College of Information Engineering, Xizang Minzu University, Xianyang 712082, China)

Abstract: In this paper, a dual-band graphene-based frequency selective surface (GFSS) is investigated and the operating mechanism of this GFSS is analyzed. By adjusting the bias voltage to control the graphene chemical potential between 0 eV and 0.5 eV, the GFSS can achieve four working states: dual-band passband, high-pass low-impedance, low-pass high-impedance, and band-stop. Based on this GFSS, a hexagonal radome on a broadband omnidirectional monopole antenna is proposed, which can achieve independent 360° six-beam omnidirectional scanning at 1.08 THz and 1.58 THz dual bands. In addition, while increasing the directionality, the peak gains of the dual bands reach 7.44 dBi and 6.67 dBi, respectively. This work provides a simple method for realizing multi-band terahertz multi-beam reconfigurable antennas.

Key words: THz antenna, multi-beam, graphene, dual-band, reconfigurable

基于石墨烯频率选择表面的双频段多波束可重构太赫兹天线

靳 钊[1], 容 瑜[1*], 乔丽萍[2*], 余景东[1], 吴 飞[1], 郭 晨[1], 田 豆[1]

(1. 长安大学 信息工程学院,陕西 西安 710064;
2. 西藏民族大学 信息工程学院,陕西 咸阳 712082)

摘要:本文研究了一种基于石墨烯的双频频率选择表面(GFSS),并分析了该GFSS的工作机理。通过调节偏置电压控制石墨烯化学势在0 eV和0.5 eV间变化,可以实现GFSS在双频段带通、高通低阻、低通高阻、带阻四种工作状态。基于此GFSS,提出了一种六边形天线罩加载在一个宽带全向单极子天线上,可以实现1.08 THz和1.58 THz双频段独立的360°六波束全向扫描。此外,在增加方向性的同时双频段的峰值增益分别达到了7.44 dBi和6.67 dBi。该工作为实现多频段太赫兹多波束可重构天线提供了一种简单的方法。

关 键 词:太赫兹天线;多波束;石墨烯;双频段;可重构

中图分类号:TN823+.25　　**文献标识码**:A

Introduction

With the increasing requirements for communication transmission rate and capacity, the utilization of existing microwave and millimeter wave bands tends to be saturated to the extent that they cannot meet the requirements of military and civilian communications, so the use of terahertz bands in wireless communications is rapidly developing[1-2]. The frequency range of terahertz waves includes the sub-millimeter wave band of 0.1-10 THz, and it is widely used in fields such as environmental monitoring, object imaging, and broadband communication due to its strong penetration, short wavelength, and rich spectral information[3-5]. One of the important components of terahertz communication networks is the terahertz antenna. Currently, various types of antennas in the terahertz band are widely studied, including microstrip antennas[6], dipole antennas[7], butterfly antennas[8], Vivaldi antennas[9], etc. Graphene is a two-di-

Received date: 2023-05-04, **revised date**: 2023-12-26　　**收稿日期**:2023-05-04,**修回日期**:2023-12-26

Foundation items: Supported by the Natural Science Foundation of Tibet Autonomous Region (XZ202401ZR0025), the National Natural Science Foundation of China (62164011, 62301081), and the Natural Science Foundation of Shaanxi Province (2022JQ-589)

Biography: Jin Zhao (1982-), Doctor of Engineering, Associate Professor, Master Supervisor. Research interests focus on microwave and antennas technology. E-mail: zhaojin@chd.edu.cn

* **Corresponding author**: E-mail: 2021224135@chd.edu.cn, lpqiao@126.com

mensional material composed of tightly arranged single-layer carbon atoms, with high thermal conductivity, high electron mobility, and other characteristics. Importantly, its surface conductivity can be controlled by changing the bias voltage applied to it[10], and based on this feature, the reconfigurable antenna loaded with graphene has been widely studied by scholars[11-16].

The reconfigurable antenna with a directional pattern can dynamically change the radiation pattern of the antenna according to the demand while ensuring the polarization mode and operating frequency band of the antenna remain unchanged, which can improve the communication capacity and security of the antenna. Ref. [11] studied a type of Yagi antenna that used a set of orthogonal dipole antennas as the feed source antenna. The beam direction can be dynamically controlled in four states through two sets of graphene-based directors and reflectors. Ref. [12] proposed an active frequency-selective surface (AFSS) by directly adding a graphene layer to the metal-dielectric structure to form a hexagonal radome, which could achieve beam steering within 360°. Ref. [13] introduced six parasitic graphene strips around the microstrip antenna, and the direction and reflection of the graphene strips could be controlled by applying electrical bias, resulting in a beam steering of 120°. Ref. [14] presented cylindrical graphene-based frequency-selective surface, which could achieve dual beam direction diagrams of front and rear radiation by placing traditional omnidirectional dipoles in the radome. Although all these antennas can achieve the radiation direction map reconstruction, they have the problem of limited beam scanning range or single operating frequency band.

In this paper, a dual-frequency multi-beam reconfigurable terahertz antenna based on GFSS is proposed. A broadband omnidirectional monopole antenna is utilized as the feed antenna and loaded with a positive hexagonal radome composed of GFSS, which divides the radiation direction equally into six 60° sections. The graphene chemical potential is controlled by the bias voltage, which can freely realize the dual-band independent directional beam steering or omnidirectional radiation within 360°. In addition, the directional radiation gain of the antenna can be further improved.

1　GFSS cell design and analysis

In this study, based on the theory of slot-type frequency selective surfaces (FSS), we designed a FSS with cross-shaped gaps distributed in the center of the unit cell and arrow-shaped gaps at the four corners. This FSS structure was engineered to generate resonance at two distinct frequencies, creating a dual-frequency bandpass filter response. To effectively harness the tunable surface conductivity of graphene, it was loaded at the locations where the electric field was concentrated on the FSS. Furthermore, to achieve independent control over the two frequency response points, we proposed a novel graphene loading method. In this method, cross shaped graphene patches were loaded beneath the cross shaped slot, while square shaped graphene patches were loaded beneath the arrow shaped slot, with both graphene patches separated from the metal layer by a dielectric material. By applying two different vertical bias voltages between the metal FSS layer and the graphene thin film layer, the chemical potential and surface conductivity of the graphene patches can be controlled. Through the individual adjustment of the direct current bias voltage on the two shapes of graphene patches, the transmission and reflection characteristics of the two pass-bands can be independently regulated, achieving independent control over the frequencies.

Figure 1 illustrates the cell structure of GFSS. The top layer consists of a cross and four arrow shaped slots with metal patches placed on the p-type silicon, and two sets of graphene structures and metal wires are added to the top and bottom of the silicon dioxide layer to connect the bias voltages. P-type silicon and silicon dioxide have dielectric constants of 11.7 and 4, respectively. This allows the surface conductivity of graphene to be controlled within a certain range and its conversion from dielectric to metallic properties. The dimensional parameters of the designed structure are listed in Table 1.

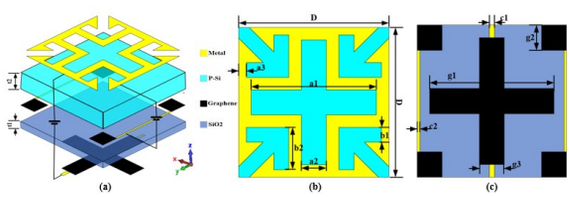

Fig. 1　Structure of GFSS unit: (a) three-dimensional structure; (b) top view, (c) bottom view
图 1　GFSS 单元结构:(a)三维结构;(b)俯视图;(c)低视图

Table 1　Antenna parameters (Unit/ μm)
表 1　天线参数(单位/ μm)

parameter	value	parameter	value	parameter	value
D	60	c2	0.05	W1	55
a1	50	g1	50	W2	4
a2	10	g2	10	L	120
a3	3	g3	10	L1	38
b1	6	t1	0.07	f	52
b2	17	t2	3	h	6
c1	0.1	W	60		

The controlled conductivity of graphene is a key property for designing reconfigurable terahertz devices, which can be expressed by the Kubo formula[10]:

$$\sigma_s = \sigma_{intra}(\omega,\mu_c,\Gamma,T) + \sigma_{inter}(\omega,\mu_c,\Gamma,T) \quad (1)$$

$$\sigma_{intra}(\omega,\mu_c,\Gamma,T) = -j\frac{e^2 k_B T}{\pi\hbar^2(\omega - j2\Gamma)}\left(\frac{\mu_c}{k_B T} + 2\mathrm{In}\left(e^{-\frac{\mu_c}{k_B T}} + 1\right)\right) \quad (2)$$

$$\sigma_{inter}(\omega,\mu_c,\Gamma,T) = -j\frac{e^2}{4\pi\hbar}\mathrm{I}\left(\frac{2|\mu_c| - (\omega - j2\Gamma)\hbar}{2|\mu_c| + (\omega - j2\Gamma)\hbar}\right), \quad (3)$$

where σ_{intra} is the intra-band conductivity, σ_{inter} is the inter-band conductivity, ω is the electromagnetic wave angular frequency, μ_c is the graphene chemical potential, $\Gamma = 2/\tau$ represents the graphene scattering rate, where τ is the relaxation time, T is the temperature, e is the electron power, $\hbar = h/2\pi$ is the approximate Planck constant, where h is the Planck constant. In fact, in the terahertz band, the surface conductivity of graphene is dominated by the intra-band conductivity, while the inter-band conductivity is negligible. In the present work, τ and T are 100 fs and 300 K, respectively. In practice, the adjustable function is usually achieved by introducing a bias voltage, and the relationship between the graphene chemical potential μ_c and the applied bias voltage V_g can be expressed as:

$$\mu_c \approx \hbar v_f \sqrt{\frac{\pi \varepsilon_0 \varepsilon_r V_g}{et}} \quad , \quad (4)$$

where V_f is the Fermi velocity of graphene, ε_r is the relative dielectric constant of the dielectric plate, and t is the thickness of the dielectric plate. In this study, the graphene layer has two distinct chemical potential states, namely 0 eV and 0.5 eV. Based on the relationship between the chemical potential and bias voltage, we can calculate that it requires a voltage of 50 V to raise the chemical potential of graphene from 0 eV to 0.5 eV. Previous research has shown that achieving lower chemical potential states in graphene can be easily accomplished through bias voltages[10, 17]. It should be noted that in practice it is more difficult to apply a DC bias voltage directly to the graphene patch, we can use a self-biased voltage source connected to the opposite pole of the voltage source to achieve reconfigurable performance for the proposed antenna[18].

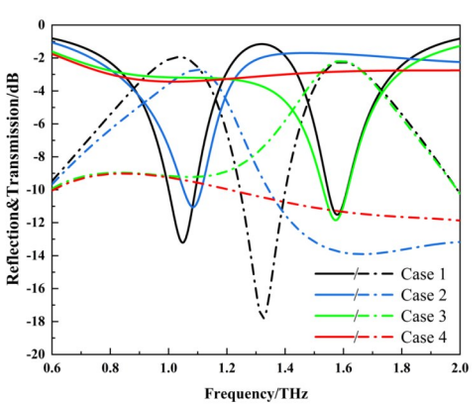

Fig. 2 Transmission and reflection characteristic curves of GFSS units
图2 GFSS单元透射和反射特性曲线

The cell structure is simulated using CST-MW to control the four rectangular graphene chemical potentials (denoted by u1) and the cross shaped graphene chemical potential (denoted by u2) switching between two states of 0 ev and 0.5 ev. Figure 2 shows the transmission and reflection curves of the proposed cell in four different graphene states when u1 and u2 are combined. When Case1, u1 and u2 are set to 0 eV, both rectangular and cross-shaped graphene exhibit dielectric properties, so the resonance occurs at each of the two points of the arrow structure and cross-structure gaps. The two resonance points occur at 1.08 THz and 1.58 THz in which bandpass effects are achieved in both frequency bands; Case2 and Case3 change u2 and u1 to 0.5 eV respectively, when controlling the chemical potential of the graphene structure to 0.5 eV, when the graphene structure in a specific frequency band behaves as a metal characteristic. By controlling u1 or u2 individually, it can effectively control whether the resonance occurs at the arrow slit and the cross-shaped slit, then low-pass high-resistance and high-pass low-resistance can be realized respectively; at Case4, both u1 and u2 are controlled to be 0.5 eV to realize the dual-band band-resistance effect. In addition, a high degree of independence can be observed at the two operating frequency points of 1.08 THz and 1.58 THz.

The surface current and electric field distribution of GFSS cell in Case2 and Case3 states are shown in Fig. 3. At 1.08 THz, the surface currents are mainly distributed at the edge of each set of arrows and the dielectric voltage is distributed in the middle of the arrows; at 1.58 THz, the surface currents are distributed at the edge of the cross and the dielectric voltage is distributed in the middle of the cross; according to the equivalent circuit, 1.08 THz and 1.58 THz correspond to an LC parallel circuit exhibiting bandpass characteristics. It is consistent with the transmission characteristics of the GFSS cell discussed earlier. Also, considering the need to construct the radome using the GFSS cell (as analyzed in Section 3), the electromagnetic wave on the GFSS cell after loading the source antenna does not always remain incident vertically. As shown in Fig. 4, when the incident wave is incident at different angles within the 40° range, the reflection and transmission characteristics still work effectively within a specific frequency band.

2 Multi-beam reconfigurable antenna loaded with GFSS

Firstly, a broadband omnidirectional monopole antenna (fed by 50 Ω) with a simple structure is proposed as a feed antenna as shown in Fig. 5. The trapezoidal patch and rectangular metal ground are placed on both sides of the dielectric substrate with the dielectric constant of 3.66 and the thickness h. The operating band contains the GFSS cell operating band, in addition, the feed antenna keeps omnidirectional radiation in the XOZ plane within the GFSS cell operating band, and the peak gain reaches 3.24 dBi and 3.53 dBi at 1.08 THz and 1.58 THz, respectively.

Then, as shown in Fig. 6, the GFSS unit is formed into a 2×3 surface around the source antenna to form a hexagonal radome. In order to analyze conveniently, we use 0 to indicate the chemical potential of 0 eV, 1 to indicate the chemical potential of 0.5 eV, then, the different chemical potential states on the hexagonal radome can be expressed using twelve binary digits, where Mode 1-6

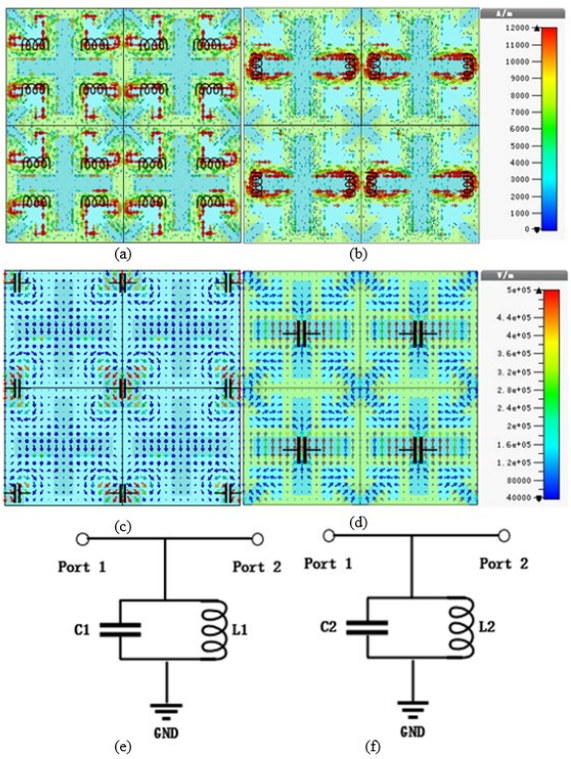

Fig. 3　Surface current, dielectric electric field distribution and equivalent circuit of the GFSS: (a), (c), (e) operates at 1.08 THz under Case 2, (b), (d), (f) operates at 1.58 THz under Case 3

图3　GFSS的表面电流、介电场分布及等效电路:(a),(c),(e)在Case 2情况时,1.08 THz谐振点,(b),(d),(f)在Case 3情况时,1.58 THz谐振点

are affected by the chemical potential of u1, which controls the low-frequency performance of the antenna; Mode 7-12 are affected by the chemical potential of u2, which controls the high-frequency performance of the antenna. The twelve working modes of the antenna after loading the hexagonal radome are shown in the table below. The antenna still maintains a good resonance at 1.08 THz and 1.58 THz for different operating modes, and the radiation direction diagrams of each mode are given, which means that the antenna loaded with GFSS radome can achieve dual-band independent 360° omnidirectional beam scanning.

Then, the antenna directionality and gain parameters in different modes after loading the radome are discussed specifically. As shown in Fig. 6(c), when the chemical potential of the graphene patches with control serial numbers 1, 2 and 3 is 0.5 eV, and the chemical potentials of the other serial numbers are 0 eV (Mode 1). Due to the increase in the chemical potential of the graphene patches, the graphene changes from a dielectric to a metallic property. At this time, the GFSS exhibits the reflective property at 1.08 THz, and therefore the radiation beam changes from omnidirectional radiation at 1. If the chemical potential of the graphene patches with serial numbers 2, 3 and 4 is 0.5 eV and the other chemical potentials are 0 eV (Mode 2), at this time the beam at 1.08 THz points at 60° and the omnidirectional radiation at 1.58 THz is maintained. Similarly, by controlling the chemical potential of the graphene patch to generate Mode 3-6, the radiation beam at 1.08 THz can be made to point to 0°, 300°, 240° and 180°, respectively, while the omnidirectional radiation characteristic at 1.58 THz is always maintained without any effect, as shown in Figs. 7(a) and 7(b) in the text. In Mode 1-6, the proposed antenna achieves a peak gain of 7.44 dBi at 1.08 THz, and the radiation gain remains within ±0.27 dBi compared to the source antenna at 1.58 THz. Similarly, Mode 7-12 are generated by varying the chemical potential of the graphene patches with control numbers 7-12, corresponding to which the radiation direction can be made to remain omnidirectional at 1.08 THz, with a minimum gain of 3.44 dBi, while the main beam is directed in each of the six directions within 360° at 1.58 THz, with a peak gain of 6.67 dBi, as shown in Figs. 7(c) and 7(d).

Furthermore, when controlling the separation of the cross-shaped and square-shaped graphene structures at 0.5 eV intervals, the hexagonal antenna enclosure exhibits its reflective characteristics at corresponding frequencies. The radiation patterns at 1.08 THz and 1.58 THz, as shown in Fig. 8, demonstrate directed three-beam ra-

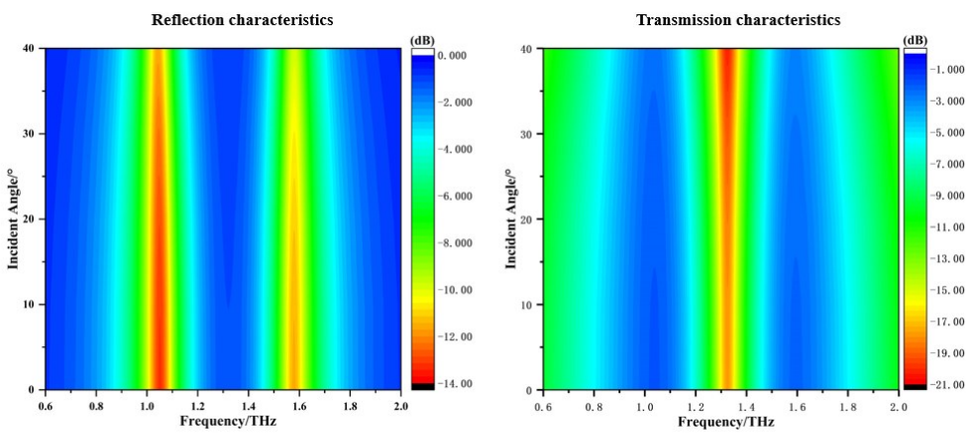

Fig. 4　Transmission/Reflection characteristics at different incidence angles

图4　不同入射角下的透射/反射特性

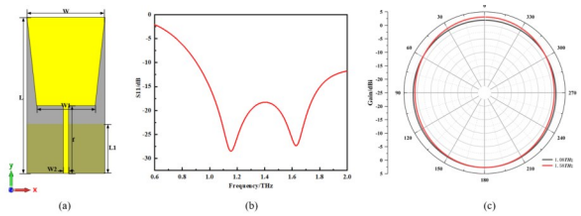

Fig. 5 Source antenna characteristics: (a) structure; (b) S parameters; (c) radiation direction of XOZ
图5 馈源天线特性:(a) 单元结构;(b) S参数;(c) XOY面辐射方向图

Table 2 List of resonance modes
表2 谐振模式列表

Mode	1	2	3	4	5	6
State	111000	011100	001110	000111	100011	110001
	000000	000000	000000	000000	000000	000000
Mode	7	8	9	10	11	12
State	000000	000000	000000	000000	000000	000000
	111000	011100	001110	000111	100011	110001

diation characteristics. This observation indicates that the proposed antenna structure possesses the capability to achieve directional beam radiation under more complex dual-frequency reflections and transmissions.

The comparison between the previously reported literature and the present work in terms of source antenna type, operating frequency, beam range and peak gain is presented below as shown in Table 3. The proposed multi-beam reconfigurable terahertz antenna based on the GFSS exhibits the capability of independently controlling six beams within a 360° coverage at dual frequencies. Additionally, it achieves high peak gains at the two resonant points.

3 Conclusions

In this paper, a GFSS radome-based multi-beam reconfigurable terahertz antenna is investigated. A graphene-based dual-band independently controllable frequency-selective surface is proposed, which is built into a hexagonal radome loaded on a monopole antenna, and the bias voltage is adjusted to control the graphene chemical potential size in the antenna to achieve the purpose of controlling the main beam direction and peak gain of the antenna. Finally, by switching two sets of graphene chemical potentials between 0 eV and 0.5 eV, the antenna can realize a dual-band independent six-beam reconfigurable antenna at 1.08 THz and 1.58 THz with peak gains of 7.44 dBi and 6.67 dBi, respectively. This work will have great prospects for applications in beam scanning of terahertz devices and systems, and gain enhancement of conventional antennas.

References

[1] Akyildiz I F, Jornet J M, Han C. Terahertz band: Next frontier for wireless communications [J]. *Physical communication*, 2014, **12**: 16-32.
[2] Mumtaz S, Jornet J M, Aulin J, *et al*. Terahertz communication for vehicular networks [J]. *IEEE Transactions on Vehicular Technology*, 2017, **66**(7).
[3] Dhillon S S, Vitiello M S, Linfield E H, *et al*. The 2017 terahertz

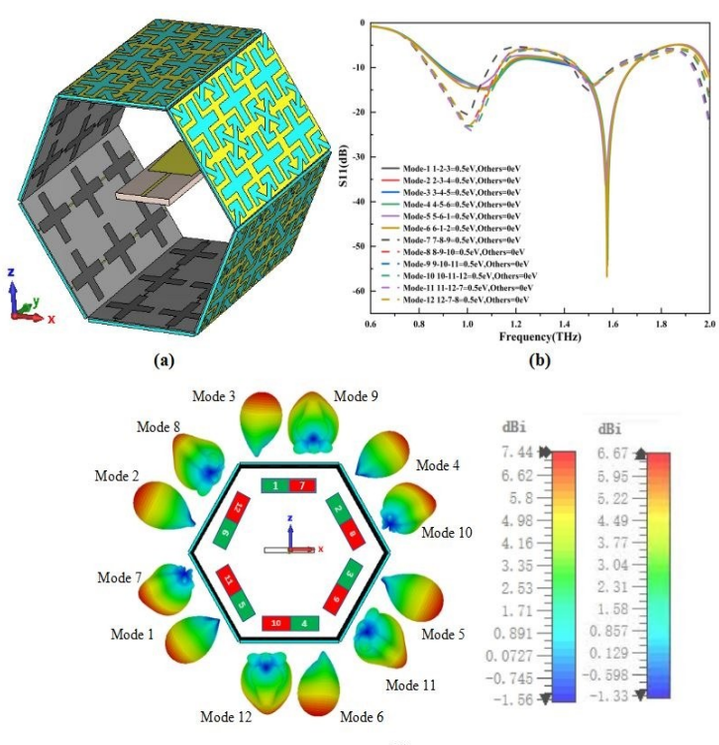

Fig. 6 Antenna characteristics of the loaded radome: (a) 3D Structure; (b) S-parameters in different modes; (c) radiation direction in different modes
图6 加载天线罩后的天线特性:(a)三维结构;(b) 不同模式下的S参数;(c)不同模式下的辐射方向图

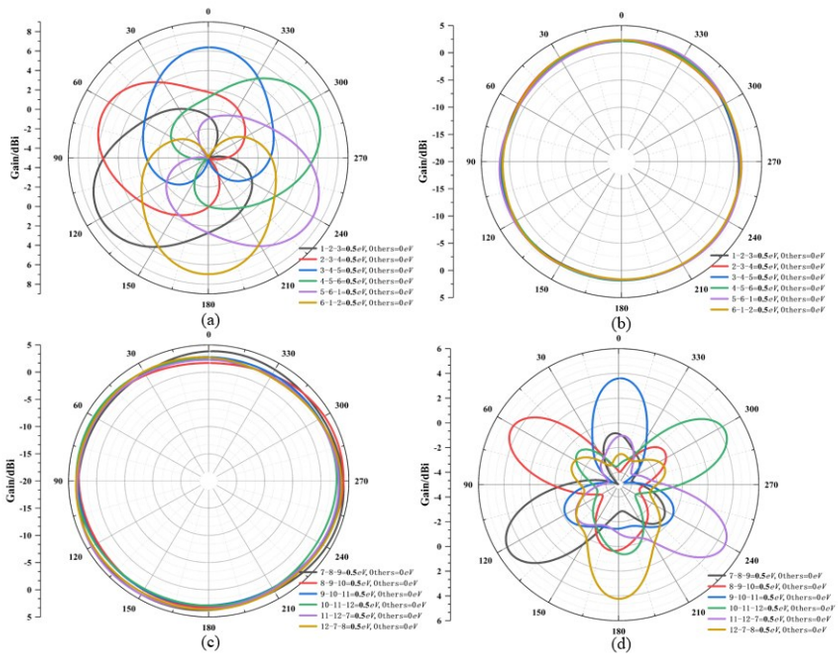

Fig. 7　Radiation direction of 1. 08 THz and 1. 58 THz: (a)-(b) Mode 1-6; (c)-(d) Mode 7-12
图7　1. 08 THz和1. 58 THz上的辐射方向图: (a)-(b)模式1-6; (c)-(d)模式7-12

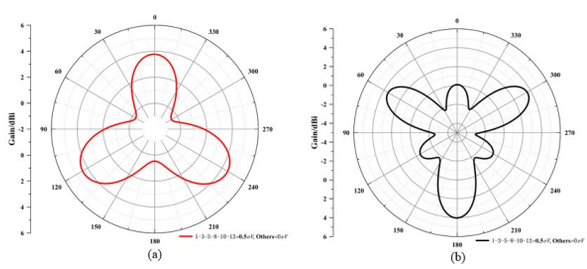

Fig. 8　Radiation direction when the interval between u1 and u2 is set to 0. 5 eV
图8　u1和u2间隔设置为0. 5 eV时的辐射方向图

Table 3　Comparison with previous literature
表3　与以往文献的比较

Reference	Source Antenna	Working frequency/THz	Beam Range	Peak Gain
Ref. [11]	Yagi Antenna	1. 8	0°, ±90°, 180°	5. 7 dBi
Ref. [12]	Monopole Antenna	1. 44	360°/ Six-beam	3. 4 dBi
Ref. [13]	Microstrip Antenna	1. 47	30°~150°	7. 91 dB
Ref. [14]	Dipole Antenna	2. 58	Two-beam	10. 11 dB
This Work	Monopole Antenna	1. 08 1. 58	360°/ Six-beam 360°/ Six-beam	7. 44 dBi 6. 67 dBi

science and technology roadmap [J]. *Journal of Physics D Applied Physics*, 2017, **50**(4): 043001.
[4] Hoeye S V, Fernandez M, Vazquez C, *et al*. Graphene Based THz Electromagnetic Imaging System for the Analysis of Artworks [J]. *IEEE Access*, 2018.
[5] Xu R, Li D, Gao S, *et al*. A Review of Broadband Low-Cost and High-Gain Low-Terahertz Antennas for Wireless Communications Applications [J]. *IEEE Access*, 2020, PP(99): 1-1.
[6] Singhal S. Ultrawideband elliptical microstrip antenna for terahertz applications [J]. *Microwave and Optical Technology Letters*, 2019, **61**(10): 2366-2373.
[7] Chashmi P K N. Reconfigurable graphene-based V-shaped dipole antenna: From quasi-isotropic to directional radiation pattern [J]. *Optik: Zeitschrift fur Licht-und Elektronenoptik: = Journal for Light- and Electronoptic*, 2019, 184.
[8] Seliuta D, Vyniauskas J, Ikamas K, *et al*. Symmetric bow-tie diode for terahertz detection based on transverse hot-carrier transport [J]. *Journal of Physics D: Applied Physics*, 2020, **53**(27): 275106 7pp).
[9] Poorgholam-Khanjari S Z F B. Reconfigurable Vivaldi THz antenna based on graphene load as hyperbolic metamaterial for skin cancer spectroscopy [J]. *Optics Communications: A Journal Devoted to the Rapid Publication of Short Contributions in the Field of Optics and Interaction of Light with Matter*, 2021, **480**(1).
[10] Hanson G W. Dyadic Green's Functions for an Anisotropic, Non-Local Model of Biased Graphene [J]. *IEEE Transactions on Antennas and Propagation*, 2008, **56**(3): 747-757.
[11] Dash S, Soni G, Patnaik A, *et al*. Switched-beam graphene plasmonic nanoantenna in the terahertz wave region [J]. *Plasmonics*, 2021, **16**: 1855-1864.
[12] Bian W, Yue H, Tong Z Y, *et al*. Large angle beam steering THz antenna using active frequency selective surface based on hybrid graphene-gold structure [J]. *Optics Express*, 2018, **26**(12): 15353-.
[13] Basiri R, Zareian-Jahromi E, Aghazade-Tehrani M. A reconfigurable beam sweeping patch antenna utilizing parasitic graphene elements for terahertz applications [J]. *Photonics and Nanostructures: Fundamentals and Applications*, 2022.
[14] Qu M, Rao M, Li S, *et al*. Tunable antenna radome based on graphene frequency selective surface [J]. *AIP advances*, 2017, **7**(9): 095307.
[15] Mabrouk A M, Seliem A G, Donkol A A. Reconfigurable graphene-based metamaterial polarization converter for terahertz applications [J]. *Optical and Quantum Electronics*, 2022, **54**(11): 769.
[16] Moradi K, Pourziad A, Nikmehr S. A frequency reconfigurable microstrip antenna based on graphene in Terahertz Regime [J]. *Optik: Zeitschrift fur Licht-und Elektronenoptik: = Journal for Light-and Electronoptic*, 2021(228-): 228.
[17] Liu M, Yin X, Zhang X. Double-layer graphene optical modulator [J]. *Nano letters*, 2012(3): 12.
[18] Gomez-Diaz J S, Moldovan C, Capdevila S, *et al*. Self-biased Reconfigurable Graphene Stacks for Terahertz Plasmonics [J]. *Nature Communications*, 2015, 6.